# REPORT ON A HELICOPTER-BORNE MAGNETIC AND ELECTROMAGNETIC SURVEY

"featuring the AeroQuest AeroTEM© System"

Bannockburn Property
Bannockburn Township, Matachewan Area, Ontario

for

MUSTANG MINERALS CORP.

Suite 302, PO Box 12
65 Queen Street West
Toronto, Ontario, M5H 2M5
Tel: (416) 955-4773 Fax: (416) 368-1539
www.mustangminerals.com

by

AEROQUEST LIMITED

4-845 Main St.
Milton, Ont., L9T 3Z3
Tel: (905) 693-9129 Fax: (905) 693-9128
www.aeroquestsurveys.com

May, 2004

## TABLE OF CONTENTS

## MAPS

The results of the survey are presented in a series of black line and colour maps at a scale of 1:10,000. Map products are as follows:

- Plate 1. Flight path with EM anomaly centres.
- Plate 2. Total Magnetic Intensity (TMI) colour grid w/line contours and anomaly centres.
- Plate 3. Z1 On-time, Z5 On-time,, and Z0 Off-time EM profiles and anomaly centres.
- Plate 4. Z0 Off-time EM colour grid w/line contours and anomaly centres.

All the maps show the flight path, claims fabric, and skeletal topography, and EM anomalies represented by conductance classified symbols. An anomaly identifier label and the estimated conductance in siemens are posted alongside the anomaly symbol. Colour contour maps show colour fill plus superimposed line contours.

## DIGITAL DATA on DVD-ROM

The results of the survey are archived on a single DVD-ROM as Geosoft GDB (binary) database(s) as well as Geosoft maps and magnetic grids. A *readme.txt* file may be found on the DVD which describes the contents in more detail.

For the reader's convenience, a copy of Geosoft's Oasis Montaj Ver 6.0 Free Interface is included on the DVD. To install the interface, unzip the two files and follow the instructions in the PDF format (Adobe Reader) guide.

The DVD also contains a digital version of this report in PDF (Adobe Acrobat) format including the technical paper by Balch, et al, which is re-printed in the appendix of this report. Adobe Acrobat Reader Ver 5.0 has been included on the DVD.

# REPORT ON A HELICOPTER-BORNE MAGNETIC AND ELECTROMAGNETIC SURVEY

Bannockburn Property

Bannockburn Township, Matachewan Area, Ontario

## 1. INTRODUCTION

This report describes a helicopter-borne geophysical survey carried out on behalf of Mustang Minerals Corp. on the Bannockburn Property, in Bannockburn Township, in the Matachewan area of Ontario.

Principal geophysical sensors included AeroQuest's exclusive AeroTEM© time domain helicopter electromagnetic system and a high sensitivity cesium vapour magnetometer. Ancillary equipment included a GPS navigation system with GPS base station, radar altimeter, video recorder, and a base station magnetometer. Raw streaming EM data, consisting of 126 channels of Z and X component sampled at 300 times per second during both on-current and off-current times, was recorded. A second RMS "analogue" acquisition system recorded 6 Z-component and one X-component channels of semi-processed EM data at 7.5 times per second, in addition to recording GPS position, magnetic field, and terrain clearance.

The Bannockburn Property was acquired by Mustang Minerals Corp. for its potential to host both economic Kambalda-style nickel-copper (Ni-Cu) mineralisation and Mount Keith-style Ni-Cu mineralisation.

Appendix 1 lists the UTM corner co-ordinates for the survey area and provides a list of claims covered by the survey. The total line kilometres (unwindowed) flown was 2368.2 km. The survey flying described in this report took place on April 20 - May 11, 2004.

Bedrock EM anomalies were interpreted and graded according to the estimated conductance. This report describes the survey, the data processing and presentation and includes an interpretation report, prepared separately by Mr. S. Balch, in the appendix.

## 2. SURVEY AREA

The Bannockburn survey block occupies the west half of Bannockburn Township,as well as parts of Montrose, Doon, Midlothian, Zavitz, Argyle and Hincks Townships. The block lies approximately 62 km south-southeast of the city of Timmins and 17 km west of the village of Matachewan (Figure 1). Primary access to the block is via Provincial Highway 566 which crosses the block in two places. Further access to the area is by numerous logging roads and trails connected to the north to Timmins and Hwy 144 and south to Shining Tree and Hwy 560. The property is centred at 48°00'N latitude, 80°55'W longitude.

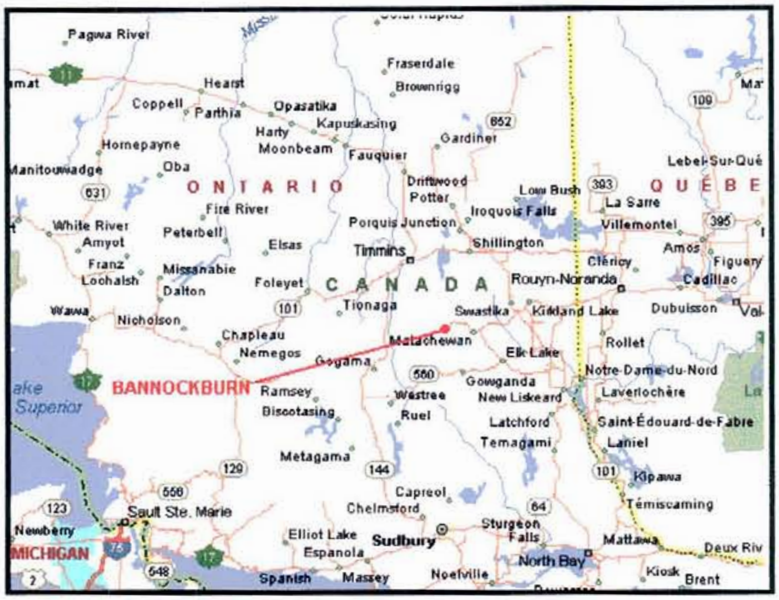


Figure 1 Regional Setting in Ontario

The Bannockburn Property consists of 79 unpatented and 12 patented mining claims covering 9250.5 hectares lying in the aforementioned townships. Of the 79 unpatented claims comprising the property, 30 are the subject of an option agreement with Outokumpu Mines Inc. and 10 are held under an option agreement with Phoenix Matachewan Mines Inc. All the claims are within the Larder Lake Mining Division except for one claim in Zavitz Township which is part of the Porcupine Mining Division. The claim block may be located on NTS 1:50,000 map sheet 41P/14 & 15, and 42A/2 & 3. The claim listing may be found in Appendix 1.

The survey crew was accommodated at the Camp Matachewan Fishing Lodge in Matachewan, Ontario. Survey specification details may be found in the next section of the report.

The physiography, geology, and history of exploration of the Bannockburn Property has been described in extensive detail in a report entitled " REPORT ON THE BANNOCKBURN NICKEL PROPERTY MATACHEWAN AREA, ONTARIO FOR MUSTANG MINERALS CORP. " by William Brereton, MPH Consulting Limited, December 1, 2003.

## 3. SURVEY SPECIFICATIONS AND PROCEDURES

The survey specifications are summarised in the following table:

| Area Name | Line Spacing (m) | Line Direction | Unwindowed Total Survey (km) | Windowed Total Survey (km) | Dates Flown (2004) |
|---|---|---|---|---|---|
| Bannockburn | 50/100 | N-S & E-W | 2368.2 | 2038.8 | Apr 25-May 11 |

The unwindowed kilometres flown is calculated by adding up the survey and control (tie) line lengths as presented in the database. The windowed kilometres is determined in the same manner but after masking the database with an outline of the claims boundary. All the survey lines flown in both the UTM grid North/South and East/West direction. The control (tie) lines were flown perpendicular to the survey lines.

Nominal EM bird terrain clearance was ~30m (100 ft). The magnetometer sensor was mounted in a smaller bird connected to the tow rope 21 metres above the EM bird and 17 metres below the helicopter. Nominal survey speed was 75 km/hr. Scan rates for data acquisition was 0.1 second for the magnetometer, electromagnetics and altimeter and 0.2 second for the GPS determined position. This translates to a geophysical reading about every 2-3 metres along flight track.

Navigation was assisted by a GPS receiver and the RMS data acquisition system which reports GPS co-ordinates as NAD27 latitude/longitude and directs the pilot over a pre-programmed survey grid. The x-y-z position of the aircraft, as reported by the GPS, is recorded at 0.2 second intervals.

Unlike frequency domain electromagnetic systems, the AeroTEM© system has negligible drift due to thermal expansion. The system static offset is removed by high altitude zero calibration lines and employing local levelling lines.

The operator was responsible for ensuring the instrument was properly warmed up prior to departure and that the instruments operated properly throughout the flight. He also maintained a detailed flight log during the survey noting the times of the flight as well as any unusual geophysical or topographic features.

On return of the aircrew to the base camp, the RMS acquisition system survey data on FlashCard was downloaded to the data processing work station. The MDAS recorded data, on removable hard-drive, was also downloaded to the processing station and archived onto DVD. In-field processing included flight preparation, transfer of the RMS acquired data to Geosoft GDB database format and production of preliminary EM, magnetic contour, and flight path maps. Survey lines which showed excessive deviation from the intended flight path were re-flown.

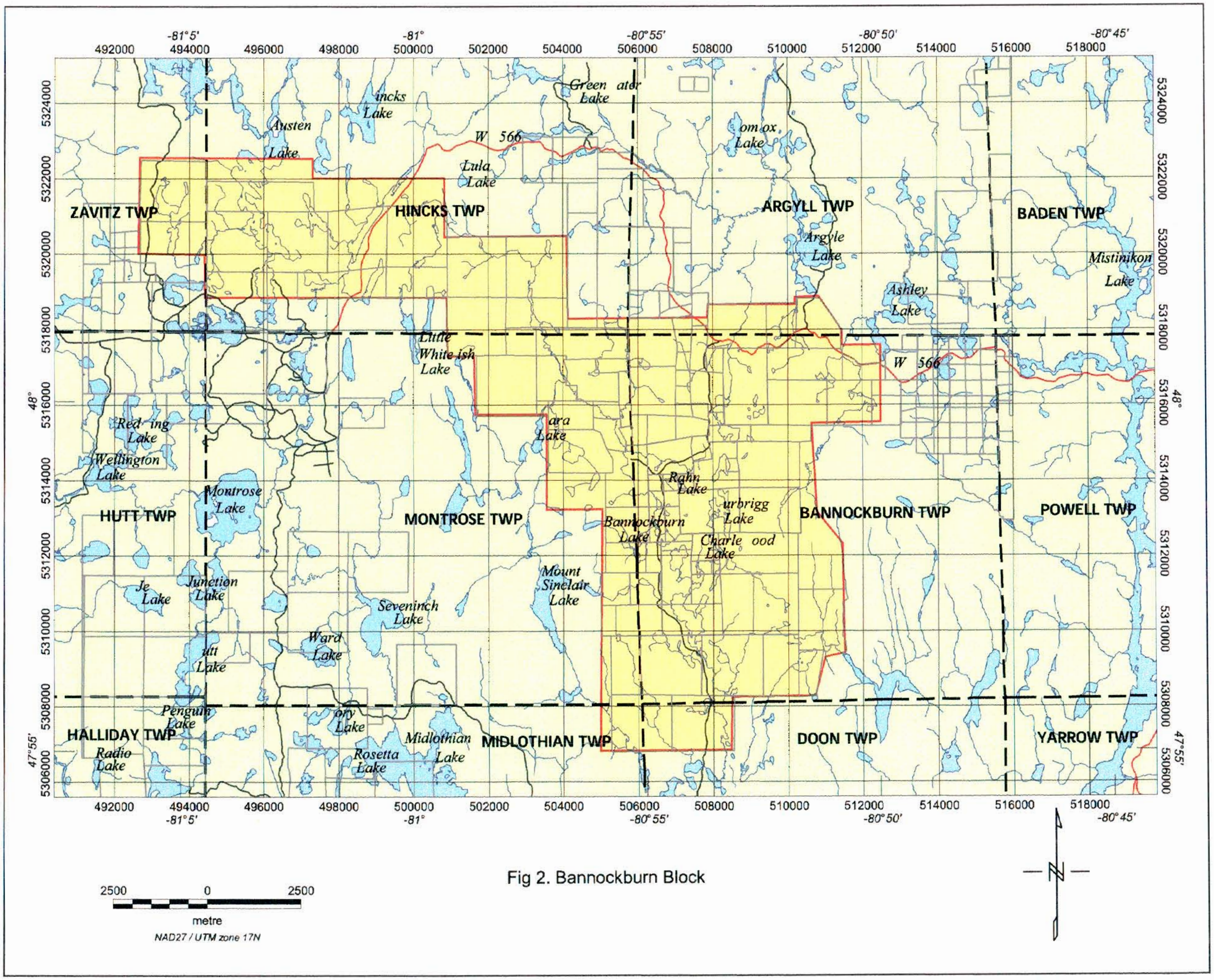


Fig 2. Bannockburn Block

# 4. AIRCRAFT AND EQUIPMENT

## 4.1 Aircraft

A Eurocopter (Aerospatiale) AS350B2 "A-Star" helicopter - registration C-FAVI was used as survey platform. The helicopters was owned and operated by Abitibi Helicopters Ltd., LaSarre, P.Q. Installation of the geophysical and ancillary equipment was carried out by AeroQuest Limited at the Gateway Helicopters Base in North Bay, Ont. then ferried to the survey area. The survey aircraft was flown at a nominal terrain clearance of 220 ft (70 m).

## 4.2 Magnetometer

The AeroQuest airborne survey system employed the Geometrics G-823A cesium vapour magnetometer sensor installed in a two metre towed bird airfoil attached to the main tow line, 17 metres below the helicopter. The sensitivity of the magnetometer is 0.001 nanoTesla at a 0.1 second sampling rate. The nominal ground clearance of the magnetometer bird was 51 metres (170 ft.). The magnetics data is recorded at 10Hz by the RMS DGR-33.

**Fig.3** The mag bird (foreground) and EM bird

### 4.3 Electromagnetic System

The electromagnetic system employed was an AeroQuest AeroTEM© Time Domain towed bird system. A triangular transmitter on-time pulse of 1.150 millisecond is employed, at a base frequency of 150 Hz. During every tx on-off cycle (300 per second), 126 contiguous channels of raw x and z component (as well as a transmitter current monitor, itx) of the received waveform are measured. Each channel width is 26.455 microsec starting at the beginning of the Tx pulse on. This 126 channel data is referred to as the raw streaming data.

Fig.4 Instrument Rack

The AeroTEM system has two separate EM data recording streams, the conventional RMS DGR-33 and the MDAS system.

**RMS DGR-33 Acquisition System**

In addition to the magnetics, altimeter and position data, six time channels of on-board real time processed off-time EM decay in the Z direction and one in the X direction are recorded by the RMS DGR-33 acquisition system at 7.5 samples per second. These channels are derived by a real-time binning, stacking and filtering procedure on the raw streaming data. The RMS data (Z1 to Z6, X1) is also sent to the analogue chart recorder and is often referred to as the analogue data.

The channel window timing of the RMS DGR-33 6 channel system is described in the table below.

| RMS Channel | Start time (microsec) | End time (microsec) | Width (microsec) | Streaming Channels | Noise tolerance |
|---|---|---|---|---|---|
| Z1, X1 | 1269.8 | 1322.8 | 52.9 | 48-50 | 20 ppb |
| Z2 | 1322.8 | 1455.0 | 132.2 | 50-54 | 20 ppb |
| Z3 | 1428.6 | 1587.3 | 158.7 | 54-59 | 15 ppb |
| Z4 | 1587.3 | 1746.0 | 158.7 | 60-65 | 15 ppb |
| Z5 | 1746.0 | 2063.5 | 317.5 | 66-77 | 10 ppb |
| Z6 | 2063.5 | 2698.4 | 634.9 | 78-101 | 10 ppb |

## MDAS Acquisition System

The 126 channels of raw streaming are recorded by the MDAS acquisition system onto a removable hard drive. The streaming data may undergo post-survey processing to yield 33 stacked and binned on-time and off-time channels at a 10 Hz sample rate. The timing of those reduced streaming channels is described in the following table.

| Processed Channel | Measured Channels | Start (microsec) | Stop (microsec) | Mid (microsec) | Width (microsec) |
|---|---|---|---|---|---|
| 1 ON | 24 | 634.9 | 661.4 | 648.1 | 26.5 |
| 2 ON | 25 | 661.4 | 687.8 | 674.6 | 26.5 |
| 3 ON | 26 | 687.8 | 714.3 | 701.1 | 26.5 |
| 4 ON | 27 | 714.3 | 740.7 | 727.5 | 26.5 |
| 5 ON | 28 | 740.7 | 767.2 | 754.0 | 26.5 |
| 6 ON | 29 | 767.2 | 793.7 | 780.4 | 26.5 |
| 7 ON | 30 | 793.7 | 820.1 | 806.9 | 26.5 |
| 8 ON | 31 | 820.1 | 846.6 | 833.3 | 26.5 |
| 9 ON | 32 | 846.6 | 873.0 | 859.8 | 26.5 |
| 10 ON | 33 | 873.0 | 899.5 | 886.2 | 26.5 |
| 11 ON | 34 | 899.5 | 925.9 | 912.7 | 26.5 |
| 12 ON | 35 | 925.9 | 952.4 | 939.2 | 26.5 |
| 13 ON | 36 | 952.4 | 978.8 | 965.6 | 26.5 |
| 14 ON | 37 | 978.8 | 1005.3 | 992.1 | 26.5 |
| 15 ON | 38 | 1005.3 | 1031.7 | 1018.5 | 26.5 |
| 16 ON | 39 | 1031.7 | 1058.2 | 1045.0 | 26.5 |
| | | | | | |
| 0 OFF | 44 | 1164.0 | 1190.5 | 1177.2 | 26.5 |
| 1 OFF | 45 | 1190.5 | 1216.9 | 1203.7 | 26.5 |
| 2 OFF | 46 | 1216.9 | 1243.4 | 1230.2 | 26.5 |
| 3 OFF | 47 | 1243.4 | 1269.8 | 1256.6 | 26.5 |
| 4 OFF | 48 | 1269.8 | 1296.3 | 1283.1 | 26.5 |
| 5 OFF | 49 | 1296.3 | 1322.8 | 1309.5 | 26.5 |
| 6 OFF | 50 | 1322.8 | 1349.2 | 1336.0 | 26.5 |
| 7 OFF | 51 | 1349.2 | 1375.7 | 1362.4 | 26.5 |
| 8 OFF | 52 | 1375.7 | 1402.1 | 1388.9 | 26.5 |
| 9 OFF | 53 | 1402.1 | 1428.6 | 1415.3 | 26.5 |
| 10 OFF | 54 | 1428.6 | 1455.0 | 1441.8 | 26.5 |
| 11 OFF | 55 | 1455.0 | 1481.5 | 1468.3 | 26.5 |
| 12 OFF | 56 | 1481.5 | 1507.9 | 1494.7 | 26.5 |
| 13 OFF | 57-60 | 1507.9 | 1640.2 | 1574.1 | 132.3 |
| 14 OFF | 61-68 | 1613.8 | 1825.4 | 1719.6 | 211.6 |
| 15 OFF | 69-84 | 1825.4 | 2248.7 | 2037.0 | 423.3 |
| 16 OFF | 85-116 | 2248.7 | 3095.2 | 2672.0 | 846.6 |

T

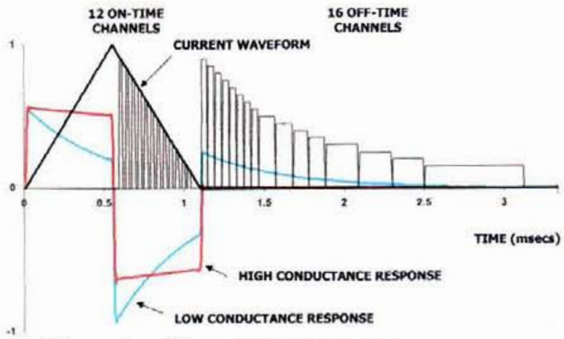


**Fig. 5** Schematic of Tx and Rx waveforms

The current AeroTEM© Transmitter Dipole moment is 38.8 kNIA. The AeroTEM© bird was towed 38 metres (125 ft) below the helicopter. More technical details of the system may be found in the technical paper in the Appendix.

## 4.4 Ancillary Systems

### Magnetometer and GPS Base Station

An integrated GPS and magnetometer base station was set up to monitor the static position GPS errors to permit differential post-processing and to record the diurnal variations of the earth's magnetic field. Each sensor, GPS and magnetic, receiver/signal processor was attached to a dedicated laptop computer for purposes of instrument control and/or data display and recording. The laptops were, in turn, linked together to provide a common recording time reference using the GPS clock.

The base magnetometer was a Scintrex CS-2 cesium precession magnetometer coupled with a Picodas MEP-710 frequency counter/decoupler. Data logging and magnetometer control was provided by the Picodas *basemag.exe* software. The logging was configured to measure at 1.0 second intervals. Digital recording resolution was 0.1 nT. The sensor was placed on a tripod away from potential noise sources outside of the lodge. A continuously updated profile plot of the base station values was available for viewing on the base station display.

The GPS base station employed a Leica Mx9212 12 channel GPS receiver with external antenna mounted near the magnetometer sensor. Although the GPS receiver was controlled by the Picodas *cdu510.exe* software, logging was not engaged as the aircraft employed a real-time differential GPS receiver. The base GPS was used only for the GPS clock for synchronisation purposes.

**RRadar Altimeter**

A Terra TRA 3500/TRI-30 radar altimeter was used to record terrain clearance. The antenna was mounted on the outside of the helicopter beneath the cockpit. The recorded data represented the height of the antenna, i.e. helicopter, above the ground. The Terra altimeter has an altitude accuracy of +/- 1.5 metres.

**Video Tracking and Recording System**

A high resolution colour VHS/8mm video camera was used to record the helicopter ground flight path along the survey lines. The video is digitally annotated with GPS position and time and can be used to verify ground positioning information and cultural causes of anomalous geophysical data.

**GPS Navigation System**

The navigation system consisted of an Ag-Nav Inc. AG-NAV2 GPS navigation system comprising a PC based acquisition system, navigation software, a deviation indicator in front of the aircraft pilot to direct the flight, a full screen display with controls in front of the operator, a Trimble AgGPS132 WAAS enabled GPS receiver mounted on the instrument rack and a Trimble antenna mounted on the magnetometer bird.

WAAS (Wide Area Augmentation System) consists of approximately 25 ground reference stations positioned across the United States that monitor GPS satellite data. Two master stations, located on either coast, collect data from the reference stations and create a GPS correction message. This correction accounts for GPS satellite orbit and clock drift plus signal delays caused by the atmosphere and ionosphere. The corrected differential message is then broadcast through one of two geostationary satellites, or satellites with a fixed position over the equator. The corrected position has a published accuracy of under 3 metres. A recent static ground test of the Trimble WAAS GPS yielded a standard deviation in x and y of under 0.6 metres and for z under 1.5 metres over a two hour period.

Survey co-ordinates are set-up prior to survey and the information is fed into the airborne navigation system. The co-ordinate system employed in the survey design was NAD83 UTM. The real-time differentially corrected GPS positional data was recorded by the RMS DGR-33 in NAD83 latitude and longitude at 0.2 second intervals directly in the analogue geophysical data file. The datum of the recorded latitude/longitude depended on the datum defined in the navigation file used to guide the survey aircraft.

### Digital Acquisition System

The RMS Instruments DGR33A data acquisition system was used to collect and record the analogue data stream, i.e. the geophysical and positional data, including processed 6 channel EM, magnetic, radar altimeter, GPS position, and time. The data was recorded on 128Mb capacity FlashCard. The RMS output was also directed to a thermal chart recorder.

The AeroTEM received waveform sampled during on and off-time at 126 channels per decay, 300 times per second, was logged in parallel by the proprietary MDAS data acquisition system. The channel sampling commences at start of the Tx cycle and the width of each channel is 26.445 microseconds. The streaming data was recorded on a removable hard-drive and was later backed-up onto DVD-ROM on the field-processing computer.

## 5. PERSONNEL

The following AeroQuest personnel were involved in the project

Field -

Party Chief: Bert Simon

Data Processor: Chris Balch

Operator: Marcus Watson

Office-

Data Processing and Report: Neil Fiset/Matt Holden/Steve Balch
Interpretation: Steve Balch

The survey pilot, Kevin Jackson, was employed directly by the helicopter operator - Abitibi Helicopters Ltd.

## 6. DELIVERABLES

The report includes a set of four geophysical maps plotted at 1:10,000 scale. The map types are as follows:

- Plate 1. Flight path with EM anomaly centres.
- Plate 2. Total Magnetic Intensity (TMI) colour grid w/line contours and anomaly centres.
- Plate 3. Z1 On-time, Z5 On-time, and Z0 Off-time EM profiles and anomaly centres.
- Plate 4. Z0 Off-time EM colour grid w/line contours and anomaly centres.

The block was divided into an A, B, and C sheet. An additional sheet, "D", covers the east-west flying with flight path and EM profiles. The basic map coordinate/projection system used to create the maps was NAD27 Canada Mean Universal Transverse Mercator Zone 17. For reference, the latitude and longitude are also noted on the maps.

All the maps show flight path trace with time reference fiducials marked at a 10 second interval, skeletal topography, claims fabric, and conductor picks represented by an anomaly symbol classified according to estimated conductance. The anomaly symbol is accompanied by postings denoting the conductance as well as an anomaly identifier label. The anomaly symbol legend may be found in the margin of the maps. Colour contour maps show colour fill plus superimposed line contours.

The geophysical profile data is archived digitally in a Geosoft GDB binary format database. The binary database contains both the processed streaming data and the RMS data.

The Geosoft database included is as follows (filename extension is "gdb"):

| Area | RMS & Streaming Data |
|---|---|
| Bannockburn | Bannockburn.gdb |

A description of the various channels found in this database may be found in the appendices of this report.

An archive CD complements the hard copy report and maps. It contains the digital database as well as the geophysical maps and grids in Geosoft format.

## 7. DATA PROCESSING AND PRESENTATION

All in-field and post-field data processing was carried out using Geosoft Montaj as well as AeroQuest proprietary data processing software. Plotting was on a 36 inch wide HP650C ink-jet plotter.

### 7.1 Base Map

The geophysical maps accompanying this report are based on positioning in the datum of NAD27 Canada Mean. The survey geodetic GPS positions have been map projected using the Universal Transverse Mercator projection in Zone 17.

A summary of the map datum and projection specifications are as follows:
Ellipse: Clark 1866
Ellipse major axis: 6378206.4m    eccentricity: 0.082271854
Datum: North American 1927 - Canada Mean
Datum Shifts (x,y,z) : 10, -158, -187 metres
Map Projection: Universal Transverse Mercator Zone 17 (Central Meridian 81°W)
Central Scale Factor: 0.9996
False Easting, Northing: 500,000m, 0m

The skeletal topography, provided by Mustang Minerals Corp., was derived from the digital Ontario Base Map (OBM) 1:20,000 map series. The claims fabric was downloaded from the MNDM website in NAD83 then reprojected to NAD27 Canada Mean before merging with the topographic data.

## 7.2 Flight Path & Terrain Clearance

The position of the survey helicopter was directed by use of the Global Positioning System (GPS). Positions were updated five times per second (5Hz) and expressed as NAD27 latitude and longitude calculated from the raw pseudorange derived from the C/A code signal.

The instantaneous GPS flight path, after conversion to NAD27 Canada Mean UTM co-ordinates, is drawn using linear interpolation between the x/y positions. The time reference fiducials are drawn on the map at appropriate intervals and are used to reference the digital data files to the plan map.

The raw Digital Terrain Mode (DTM) was derived by simply taking the satellite position altitude and subtracting the radar altimeter. The calculated values are relative and are not tied into to surveyed geodetic heights.

## 7.3 Electromagnetic Data

The raw streaming data, sampled at a rate of 38,400 Hz (126 channels, 300 times per second) was reprocessed using a proprietary software algorithm developed by Mr. Steve Balch. Processing began with a segmenting and synchronisation procedure that isolates the relevant portion of the flight and pre-processes the time series to ensure data synchronisation is maintained. The pre-processed segment was then partially stacked and tested for high noise events, including sferics, which are skipped during the main stacking procedure. The coefficients for the waveform deconvolution process were also determined.

During the main processing algorithm, data were stacked for 40 full-cycles or 0.2 seconds. Deconvolution of the system waveform, primary field removal during the on-time, and system transient removal during the off-time were performed ahead of the stacking. The data were then binned into the 16 On-time and 17 Off-time channels and their base levels corrected. The resulting profiles were then filtered using a filter with 11 coefficients. An overburden stripped response was generated by subtracting the off-time response from the on-time response for the X1 to X16 and Z1 to Z16 channels.

The final processing step was to merge the processed EM data back into a Geosoft GDB file with the GPS position, altimeter, levelled magnetics, etc. data. The EM fiducial is used to synchronise the two datasets. The processed channels are labelled in the database as ZOn1 to ZOn16, ZOff0 to ZOff16, XOn1 to XOn16, and XOff0 to XOff16. The overburden stripped channels are labelled Z1Obr to Z16Obr and X1Obr to X16Obr. In the database, the processed AeroTEM EM channels are expressed as nT/sec. To convert to parts per billion (ppb), multiply by 6.96. Conductors were interpreted based on a close visual examination of the EM profiles and taking into account the magnetic data along with geological and geochemical data provided by the client. A report of that interpretation may be found in the Appendices.

Conductors were interpreted based on a close visual examination of the EM profiles and taking into account the magnetic data along with geological and geochemical data provided by the client. A report of that interpretation may be found in the Appendices.

At each conductor pick, the on-time and off-time conductance have been calculated based on a conventional vertical thin sheet model and where the channel response satisfies a threshold of 5.0 nT/s on-time and 2.5 nT/s off-time. From these calculated values, an interpreted conductance (COND) value has been assigned to each anomaly. The assigned value is determined from the off-time response, unless there are 16 off-time channels with nT/s >2.0 in the response. In that event the assigned value is taken from the on-time because of the higher conductance. In the case of conductors marked by a double peak type response (thin, shallow sources) where the EM coupling is a minima over or near the conductor axis, the conductance value (COND) is derived from the higher response area adjacent to the axis. For each interpreted conductor, the number of off-time channels of response (from channels ZOff1-ZOff16) above the threshold is also noted.

Each conductor pick has been given an identification letter label and has also been classified according to a set of seven ranges of conductance values. The anomalies were then plotted on the plan maps with one of seven symbols reflecting that classification level. Adjacent to the map symbol is posted the identifier label as well as the interpreted conductance values in siemens. The maximum possible number of off-time channels is 16 given the first channel of the 17 processed channels is not included.

With regard to the six channel off-time data recorded by the RMS DGR-33, after a lag correction then a two stage digital filtering process was used to remove any residual short wavelength noise. Sharp large amplitude events were removed with a 0.4 sec non-linear filter. The signal to noise ratio was further improved by the application of a low pass linear digital filter. This filter has zero phase shift which prevents any lag or peak displacement from occurring, and it suppresses only variations with a wavelength less than about 1.0 seconds or 30 metres. This filter is referred to as a 1.0 sec linear filter. The raw channels are denoted in the database with the suffix "raw", e.g. z1raw, x1raw, etc. The filtered channels are indicated by the "f" suffix, e.g.. z1f, x1f, etc.

During the high elevation checks, an internal 5 second wide calibration pulse in all EM channels was generated in order to ensure that the gain of the system remained constant and within specifications.

## 7.4 Magnetic Data

Prior to any levelling the magnetic data was subjected to a lag correction of -0.1 seconds and a spike removal filter. The filtered aeromagnetic data were then corrected for diurnal variations using the magnetic base station and the intersections of the tie lines. No corrections for the regional reference field (IGRF) were applied. The corrected profile data were interpolated on to a grid using a random grid technique with a grid cell size of 25 metres. The final levelled grid provided the basis for threading the presented contours which have a minimum contour interval of 20 nT.

Respectfully submitted,

Neil Fiset, B.Sc.,
AeroQuest Limited
August 18, 2004

## APPENDIX 1

Interpretation Report by S. Balch

INTERPRETATION REPORT

# Summary of an AeroTEM Airborne Geophysical Survey

# On the Bannockburn Property

# For

# Mustang Minerals Corp

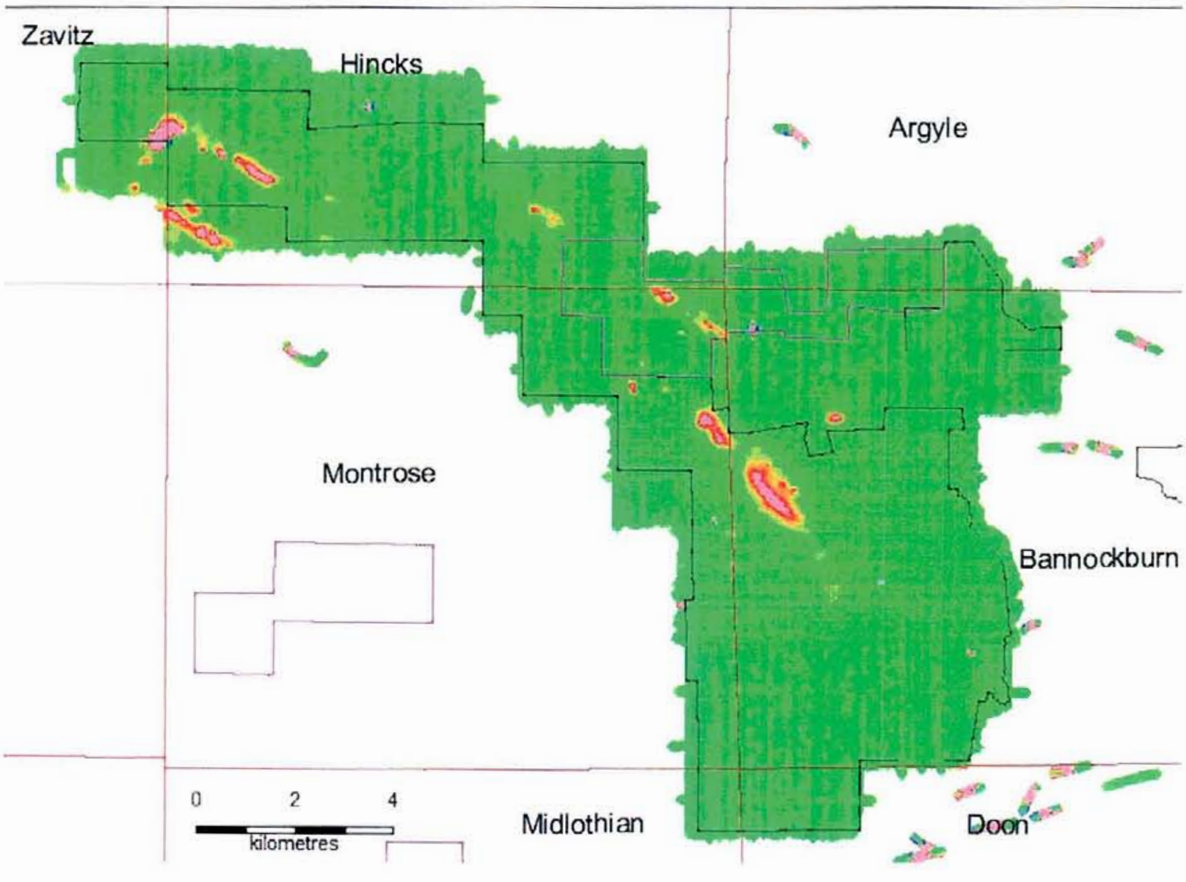


By

S.J. Balch

June 20, 2004

## Introduction

Aeroquest Limited flew an AeroTEM helicopter electromagnetic and magnetometer survey over the Bannockburn Property owned by Mustang Minerals Corp during May and June of 2004. The main purpose of the survey was to characterize the nickel-copper-precious metals (Ni-Cu-PGMs) intersections of the known mineralization and to detect new Ni-Cu-PGM mineralization. The second purpose of the survey was to identify any other conductive targets that have the potential to be a mineralizing system and to characterize these targets as well.

The AeroTEM survey comprised a total of 2450 line kilometres. Over the known mineralization the line spacing was 50 m in both directions. Over the remainder of the property the line spacing was 100 m in a north to south line direction.

## Background

Mustang Minerals Corp (Mustang) is exploring for Ni-Cu-PGM mineralization within ultramafic flows that are often termed Kambalda-type komatiitic lava flows. The geologic model assumes that nickel-sulphide within the ultramafic flow can erode the base of the host rock to form thickened zones of massive sulphide. This is a primary exploration target. It is also possible for nickel-sulphide to invade the country rock as veins or splays. This is also a primary exploration target. Lower percent nickel-sulphide can also occur within the ultramafic host. If the nickel tenor is high enough, it is possible to have economic concentrations within the host without requiring the concentration mechanisms of erosion or splaying. This is a secondary exploration target.

The geophysical signatures of Kambalda-type Ni-Cu-PGM mineralization will vary depending upon the nature of the target, but there are three general models that closely follow the geological ones. The most common model is a target of high conductance occurring within an area of highly anomalous magnetic field. The assumption is that the nickel-sulphide is highly conductive and occurs within the highly magnetic ultramafic. The second geophysical model is a high conductance target without an associated magnetic field high, but close to one. Here the geological model is massive nickel-sulphide splays that have exited the ultramafic host and entered the country rock. The third geophysical model is broad conductive trends that occur within a strong magnetic field high. This is the ultramafic host model with elevated nickel-sulphide where the concentration of sulphide is relatively low but the nickel tenor is elevated.

## Results

At Bannockburn, AeroTEM has identified magnetic and conductive trends that satisfy two of the three geological models. In addition a number of interesting targets have been identified that are unlikely to represent nickel-sulphide within an ultramafic host, but nonetheless are of great interest. All of the targets are described below by zone.

The total magnetic field image is shown in Figure 1 for the entire property. An early time Z-axis EM response is shown in Figure 2. The total number of conductive trends on the property is estimated to be about 12 depending on how the trends are subdivided. This range provides an excellent framework for follow-up because the target areas are well defined.

## B-Zone

The B-Zone is characterized by low percent sulphide within an ultramafic flow that extends for a distance of 1.2 km. The zone averages 1-2 S of conductance and appears to be rather uniform throughout. On some lines the conductance (and also the amplitude) increases slightly at the margins of the ultramafic suggesting a slight enhancement of sulphide at the contact, but in general the center of the ultramafic shows the highest conductance. The magnetic field over the B-Zone is shown in Figure 3, while the mid on-time EM response is shown in Figure 4. AeroTEM on-time profiles are shown in Figure 5 along with the total magnetic field and estimated conductance. The average conductance of the B-Zone at 1-2 S extends across distances of 200 m or more. This puts an estimate for conductivity of less than 0.01 S/m (10 ohm-m). Despite the high amplitude responses noted in the AeroTEM (and previous MegaTEM) survey, the B-Zone is a relatively poor conductor. The center of the B-Zone is listed in Table 1 for the east-west AeroTEM flight lines. Boreholes drilled in the vicinity of lines 3380 to 3431 would test the typical style of mineralization within the B-Zone. The possibility of an economic deposit would be tied more to a change in the sulphide tenor than to an increase in sulphide content (and hence an increase in metal concentration).

| Line | Conductance (S) | East (m) | North (m) | Comments |
|---|---|---|---|---|
| 3230 | 0.67 | 506376 | 5314467 | North limit of B-Zone. Mineralization on eastern side of ultramafic. |
| 3241 | 0.63 | 506362 | 5314437 | Mineralization of eastern side of ultramafic. |
| 3250 | 1.22 | 506336 | 5314373 | Mineralization extends throughout ultramafic. |
| 3262 | 1.06 | 506380 | 5314332 | Mineralization centered within ultramafic. |
| 3270 | 1.07 | 506322 | 5314263 | Conductance rises near edges of zone. |
| 3280 | 1.24 | 506345 | 5314226 | |
| 3290 | 1.17 | 506342 | 5314183 | Conductance highest in center of ultramafic. |
| 3300 | 1.36 | 506332 | 5314128 | Broad zone of conductance with magnetics. |
| 3310 | 1.42 | 506345 | 5314076 | Broad zone of conductance with magnetics. |
| 3320 | 1.65 | 506375 | 5314026 | Broad zone of conductance with magnetics. |
| 3330 | 1.67 | 506359 | 5313981 | Broad zone of conductance with magnetics. |
| 3340 | 2.03 | 506380 | 5313928 | Broad zone of conductance with magnetics. |
| 3350 | 1.81 | 506433 | 5313882 | Broad zone of conductance with magnetics. |
| 3360 | 1.83 | 506480 | 5313827 | Broad zone of conductance with magnetics. |
| 3372 | 2.01 | 506553 | 5313779 | Broad zone of conductance with magnetics. |
| 3380 | 2.22 | 506569 | 5313729 | Broad zone of conductance with magnetics. |
| 3390 | 2.40 | 506613 | 5313673 | Broad zone of conductance with magnetics. |
| 3400 | 2.15 | 506629 | 5313620 | Broad zone of conductance with magnetics. |
| 3410 | 2.21 | 506663 | 5313579 | Broad zone of conductance with magnetics. |
| 3420 | 2.11 | 506674 | 5313538 | Broad zone of conductance with magnetics. |
| 3431 | 2.07 | 506750 | 5313479 | Broad zone of conductance with magnetics. |
| 3440 | 1.85 | 506759 | 5313437 | Broad zone of conductance with magnetics. |
| 3450 | 1.85 | 506712 | 5313382 | Broad zone of conductance with magnetics. |
| 3460 | 1.54 | 506968 | 5313324 | Broad zone of conductance with magnetics. |
| 3470 | 1.51 | 506944 | 5313276 | Broad zone of conductance with magnetics. |
| 3480 | 1.15 | 506952 | 5313225 | Broad zone of conductance with magnetics. |
| 3490 | 1.12 | 507064 | 5313169 | Broad zone of conductance with magnetics. |
| 3500 | 0.95 | 507143 | 5313128 | Broad zone of conductance with magnetics. |
| 3510 | 0.90 | 507219 | 5313084 | Broad zone of conductance with magnetics. |
| 3520 | 1.77 | 507075 | 5313031 | Obvious trend of increasing conductance to the west at depth. |

| | | | | |
|---|---|---|---|---|
| 3530 | 1.70 | 507180 | 5312974 | Obvious trend of increasing conductance to the west at depth. |
| 3540 | 2.31 | 507165 | 5312927 | South termination of B-Zone. |

***Table 1. B-Zone conductor picks.***

## B-Zone Splay

The B-Zone splays into a small secondary zone at the southwest margin of the ultramafic unit. Based on the low conductance valuess (ranging from 0.40 to 1.24 S) it is unlikely that higher grade mineralization would be intersected within this splay. The approximate axis of the B-Zone splay is summarized in Table 2.

| Line | Conductance (S) | East (m) | North (m) | Comments |
|---|---|---|---|---|
| 3460 | 0.97 | 506538 | 5313327 | Low conductance splay of the B-Zone. |
| 3470 | 0.97 | 506559 | 5313262 | Low conductance splay of the B-Zone. |
| 3481 | 0.80 | 506553 | 5313233 | Low conductance splay of the B-Zone. |
| 3490 | 0.93 | 506606 | 5313191 | Low conductance splay of the B-Zone. |
| 3500 | 1.24 | 506682 | 5313138 | Low conductance splay of the B-Zone. |
| 3510 | 0.40 | 506577 | 5313080 | Low conductance splay of the B-Zone. |

***Table 2. B-Zone splay conductor picks.***

## C-Zone

The C-Zone shows the highest conductance of any of the targets within the main ultramafic under exploration within the Bannockburn Property. On line 3380, for example, the peak conductance is 7 S, still low for pyrrhotite-rich massive sulphide, but much higher than the B-Zone. Given the narrow intersections of the C-Zone relative to the B-Zone, the conductivity of the C-Zone ranges from 0.1-1.0 S/m, or from ten to one hundred times greater than that of the B-Zone.

The C-Zone was flown with both north-south and east-west flight lines. Although the mineralization is thought to be trending east-west, the responses from the east-west flight lines produce a higher conductance and appear to be more diagnostic. A likely explanation is that flight line 3380 is located directly over the axis of the C-Zone. But it might also be possible that the C-Zone mineralization has both an east-west component and one that is north-south. It is recommended that the conductor picks be more closely matched to the geology and that some drilling be considered in an east-west direction to test for a possible north-south orientation to the mineralization. If the C-Zone is fault controlled there could be portions of the mineralization located along the fault margins (that are proposed to be oriented north-south).

| Line | Conductance (S) | East (m) | North (m) | Comments |
|---|---|---|---|---|
| 3372 | 2.54 | 507220 | 5313775 | Emergence of C-Zone on east-west lines. No magnetic association. |
| 3380 | 7.03 | 507165 | 5313732 | Higher conductance response. |
| 3390 | 2.89 | 507121 | 5313674 | Edge of C-Zone. |
| 1450 | 1.56 | 507067 | 5313697 | Should be surrounded by low percent sulphide. |
| 1455 | 2.48 | 507116 | 5313720 | Slight north dip. |
| 1460 | 2.58 | 507168 | 5313696 | Thin sub-vertical response. |
| 1465 | 2.99 | 507219 | 5313758 | Small discrete response. |

| | | | | |
|---|---|---|---|---|
| 1470 | 2.61 | 507267 | 5313664 | Very deep response (100+ m). |

***Table 3. C-Zone conductor picks.***

## D-Zone

The D-Zone is likely related to low percent sulphide located along the eastern margin of the ultramafic unit. There appear to be 2 zones defining this trend with an interruption between flight lines 3300 and 3330. The conductance range of the D-Zone is 0.12-1.41 S. Given its smaller thickness relative to the B-Zone the mineralization of the D-Zone is probably similar and would give rise to a similar conductivity. No drilling recommendations can be made with regards to the D-Zone unless there is a possibility that the nickel tenor is greater along the eastern margin of the ultramafic. Conductor picks for the D-Zone are listed in Table 4.

| Line | Conductance (S) | East (m) | North (m) | Comments |
|---|---|---|---|---|
| 3262 | 0.38 | 506938 | 5314322 | North limit of D-Zone |
| 3270 | 0.12 | 506922 | 5314264 | Conductor centered within ultramafic splay. |
| 3280 | 0.16 | 506911 | 5314228 | Centered within magnetic response. |
| 3290 | 0.12 | 506935 | 5314179 | Probable pinching of the mineralization. |
| 3300 | 0.78 | 506915 | 5314132 | Lower amplitude, higher conductance. |
| 3330 | 0.85 | 506901 | 5313975 | Re-emergence of D-Zone. |
| 3340 | 0.74 | 506867 | 5313927 | D-Zone. |
| 3350 | 0.85 | 506898 | 5313863 | D-Zone. Strong magnetic association. |
| 3360 | 0.73 | 506904 | 5313831 | D-Zone. Strong magnetic association. |
| 3372 | 1.19 | 506968 | 5313778 | D-Zone conductance up marginally. |
| 3380 | 1.41 | 506958 | 5313735 | D-Zone amplitude dropping. |

***Table 4. D-Zone conductor picks.***

## I-Zone

The I-Zone is not related to nickel sulphide within an ultramafic. The zone is best described as having an east to west strike direction (300 m), moderate conductance, and no magnetic association. The eastern limit of the trend appears to be the most conductive (8-10 S). Lines 1540-1545 have the highest amplitude. Ground prospecting is recommended on the latter two lines, with a possible drill target suggested near 1545-1555 if the area is thought to be favourable for VMS style mineralization.

| Line | Conductance (S) | East (m) | North (m) | Comments |
|---|---|---|---|---|
| 1525 | 1.86 | 507815 | 5315218 | Moderate conductance target with no magnetic association. |
| 1530 | 1.60 | 507867 | 5315225 | Thin conductor dipping to the south, low conductance and no magnetic association. |
| 1535 | 1.37 | 507921 | 5315227 | Two closely spaced conductors with no magnetic association. |
| 1540 | 4.07 | 507966 | 5315235 | Good amplitude, moderate conductance target, showing current migration to the south, with no magnetic association. |
| 1545 | 5.32 | 508018 | 5315233 | Good amplitude, moderate conductance target, |

| | | | | |
|---|---|---|---|---|
| | | | | showing current migration to the south, with no magnetic association. |
| 1550 | 8.27 | 508070 | 5315224 | Moderate amplitude, good conductance target, thick, no magnetic association. |
| 1555 | 10.65 | 508122 | 5315229 | Moderate amplitude, good conductance target, no magnetic association. |
| 1560 | 3.21 | 508164 | 5315231 | Low amplitude, low conductance target representing the eastern termination of the I-Zone, with no magnetic association. |

***Table 5. I-Zone conductor picks.***

**J-Zone**

The J-Zone is a southeast trending conductor that dips to the northeast and extends from flight lines 1170 to 1320. The zone has no magnetic association. To the northwest the zone is dipping steeply to the northeast and is thin. Toward the southeast the zone dips to the northeast at a shallow angle (within 30° of surface). The cause for the conductor is unknown, but it has the same trend as the main ultramafic unit at Bannockburn.

| Line | Conductance (S) | East (m) | North (m) | Comments |
|---|---|---|---|---|
| 1170 | 0.50 | 504268 | 5317707 | Low conductance target dipping to the northeast. |
| 1180 | 0.64 | 504366 | 5317679 | Low conductance target dipping to the northeast. |
| 1190 | 1.69 | 504469 | 5317663 | Low conductance target dipping to the northeast. |
| 1200 | 1.29 | 504560 | 5317622 | Low conductance target dipping to the northeast. |
| 1210 | 1.29 | 504668 | 5317616 | Low conductance target dipping to the northeast. |
| 1220 | 0.27 | 504766 | 5317522 | Low conductance target dipping to the northeast, very low amplitude. |
| 1240 | 0.13 | 504966 | 5317462 | Low conductance target dipping to the northeast, very low amplitude. |
| 1250 | 0.18 | 505076 | 5317375 | Low conductance target, thin and possibly sub-vertical, very low amplitude. |
| 1260 | 0.09 | 505175 | 5317322 | Low conductance target, thin and possibly sub-vertical or south dipping, very low amplitude. |
| 1270 | 0.76 | 505266 | 5317232 | Low conductance target, thin and possibly sub-vertical or south-dipping, very low amplitude. |
| 1280 | 1.17 | 505370 | 5317131 | Low conductance target dipping to the northeast, very low amplitude. |
| 1290 | 3.00 | 505471 | 5317001 | Moderate conductance target, dipping at a shallow angle to the northeast. Conductor pick represents upper edge. |
| 1300 | 2.61 | 505566 | 5316947 | Moderate conductance target, dipping at a shallow angle to the northeast. Conductor pick represents upper edge. |

| | | | | |
|---|---|---|---|---|
| 1310 | 2.93 | 505664 | 5316870 | Moderate conductance target, dipping at a shallow angle to the northeast. Conductor pick represents upper edge. |
| 1320 | 3.09 | 505768 | 5316873 | Moderate conductance target, dipping at a shallow angle to the northeast. Conductor pick represents upper edge. |

***Table 6. J-Zone conductor picks.***

**K-Zone**

The K-Zone is a trend of conductors with little or no magnetic association, oriented southeast and having low conductance. The conductor is dipping to the northeast, often at a shallow angle. Ground prospecting is suggested to explain this feature. It appears to be along strike of the J-Zone conductor.

| Line | Conductance (S) | East (m) | North (m) | Comments |
|---|---|---|---|---|
| 920 | 0.33 | 501765 | 5319449 | North dipping conductor, thin, low conductance, with low amplitude magnetic field response. |
| 930 | 1.65 | 501866 | 5319351 | Conductor dipping at a shallow angle to the north, having low conductance and magnetic association (low amplitude). Pick represents upper edge of conductor. |
| 940 | 2.14 | 501967 | 5319334 | Conductor dipping at a shallow angle to the north, having low conductance and magnetic association (low amplitude). Pick represents upper edge of conductor. |
| 950 | 1.37 | 502069 | 5319290 | Conductor dipping at a shallow angle to the north, having low conductance and magnetic association (low amplitude). Pick represents upper edge of conductor. EM response has very low amplitude. |
| 960 | 1.20 | 502168 | 5319251 | Sub-vertical to north dipping, thin conductor with no magnetic response. |
| 970 | 1.37 | 502263 | 5319221 | Sub-vertical to north dipping, thin conductor with no magnetic response. |
| 980 | 1.78 | 502369 | 5319120 | Conductor dipping at a shallow angle to the north, having low conductance and magnetic association (low amplitude). Pick represents upper edge of conductor. EM response has very low amplitude. |
| 990 | 1.09 | 502464 | 5319125 | Weak amplitude target having low conductance and no magnetic association. |
| 1000 | 1.26 | 502567 | 5319120 | Weak amplitude target having low conductance and no magnetic association. |

***Table 7. K-Zone conductor picks.***

## L-Zone

The L-Zone is a shallow, moderate conductance target that dips to the northeast. The zone strikes to the southeast and is sub-parallel to the J- and K-zones. It is possible that the shallow dipping conductors, such as the L-Zone, represent sedimentary cover and are not bedrock conductors. This possibility should be reviewed because most of the shallow dipping conductors have the same strike direction, and could be formational.

| Line | Conductance (S) | East (m) | North (m) | Comments |
|---|---|---|---|---|
| 330 | 4.0 | 495865 | 5320375 | Northeast dipping. |
| 340 | 3.0 | 495970 | 5320297 | Northeast dipping sheet. |
| 350 | 2.1 | 496070 | 5320217 | 25 m estimated depth. |
| 360 | 3.0 | 496175 | 5320099 | Northeast dipping, no magnetic association. |
| 370 | 1.7 | 496264 | 5320075 | 50 m estimated depth. |
| 380 | 7.4 | 496374 | 5320020 | 50 m estimated depth. |
| 390 | 6.7 | 496469 | 5319984 | 35 m estimated depth. |
| 400 | 3.0 | 496573 | 5319936 | 75 m estimated depth. |
| 410 | 2.2 | 496670 | 5319923 | 100 m estimated depth. |

***Table 8. L-Zone conductor picks.***

## M-Zone

The M-Zone is a high-amplitude, good conductance target that shows considerable thickness on some flight lines (e.g. 180). The strike direction is to the northeast on the western lines, and southeast on the eastern lines suggesting a possible fold nose. The northeast trending portion has an associated magnetic response while the southeast trending portion does not. The zone could represent two conductor trends, in which case the northeast trending section of the western most lines is of greater interest, owing to its apparent thickness, and magnetic association.

| Line | Conductance (S) | East (m) | North (m) | Comments |
|---|---|---|---|---|
| 210 | 12.5 | 494670 | 5321037 | Shallow (~25 m) dipping to the north steeply. |
| 200 | 14.2 | 494568 | 5321087 | North dipping, magnetic association, two conductors present. |
| 190 | 30.6 | 494472 | 5321061 | 50 m estimated depth. |
| 190 | 57.6 | 494468 | 5321211 | |
| 180 | 45.4 | 494370 | 5320951 | <25 m below surface. |
| 180 | 18.0 | 494368 | 5321198 | 65 m estimated depth. |
| 170 | 43.0 | 494270 | 5320877 | <20 m below surface. |
| 160 | 35.0 | 494165 | 5320802 | <20 m below surface. |
| 150 | 27.7 | 494073 | 5320847 | 60 m estimated depth, dipping north. |

***Table 9. M-Zone conductor picks.***

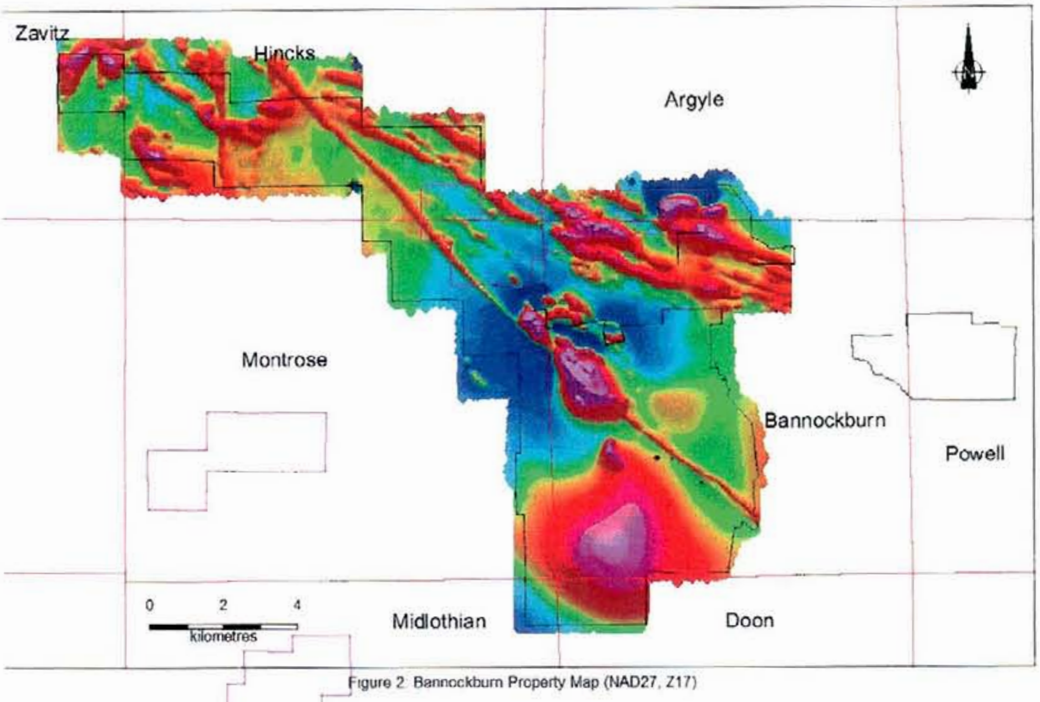


Figure 1. Total magnetic field over the Bannockburn Property.

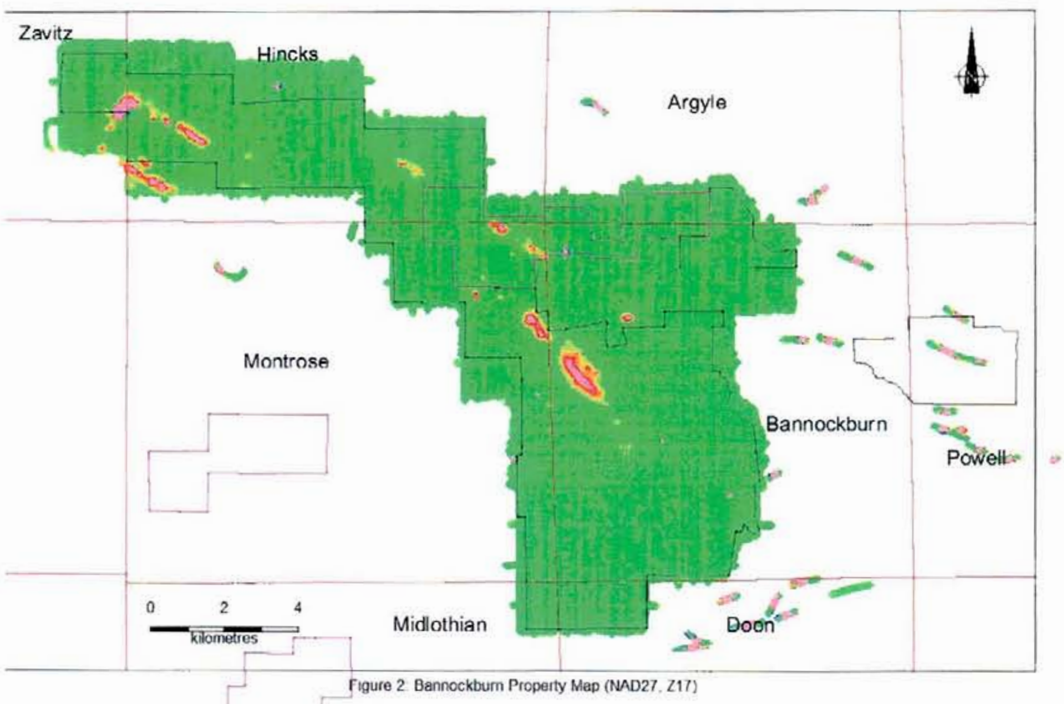


Figure 2. Mid time-channel (channel 7) on-time EM response, Bannockburn Property.

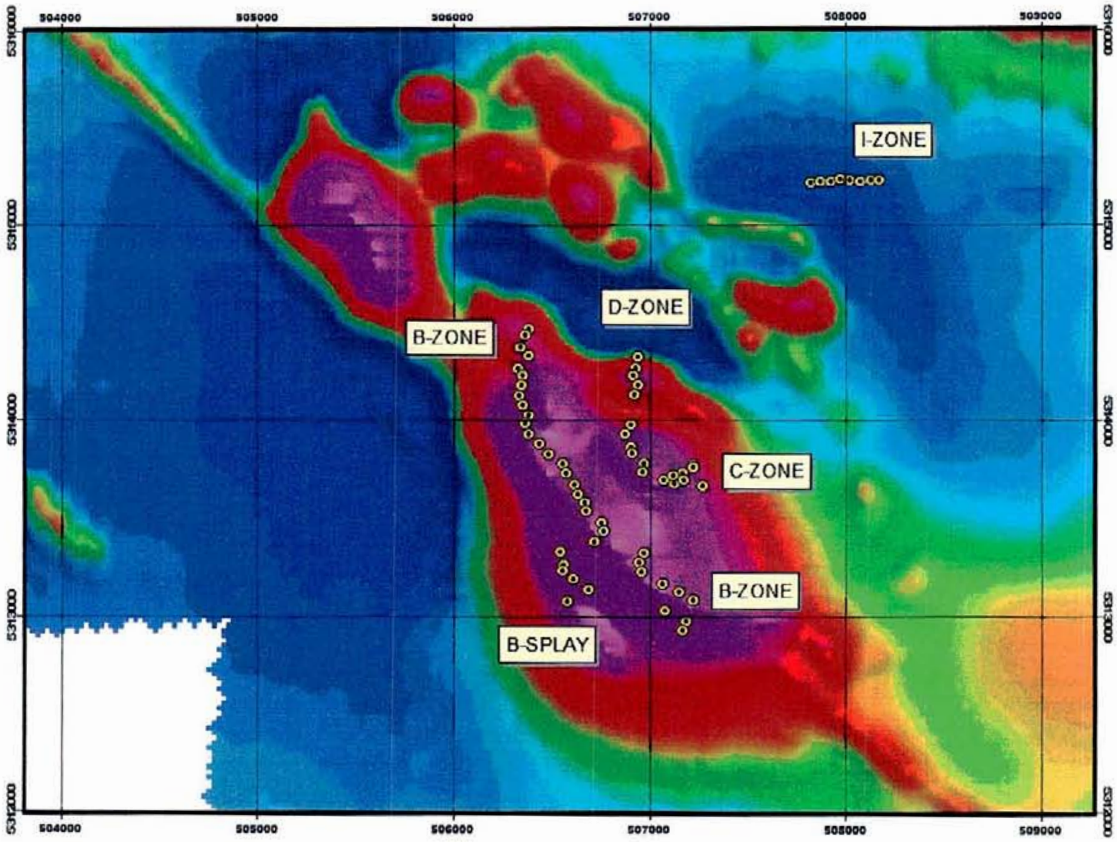


Figure 3. The B-Zone at Bannockburn is a conductive trend oriented along the central axis of a strongly magnetic ultramafic unit. To the northeast are the D- and C-Zones. To the southwest is the B-Zone splay.

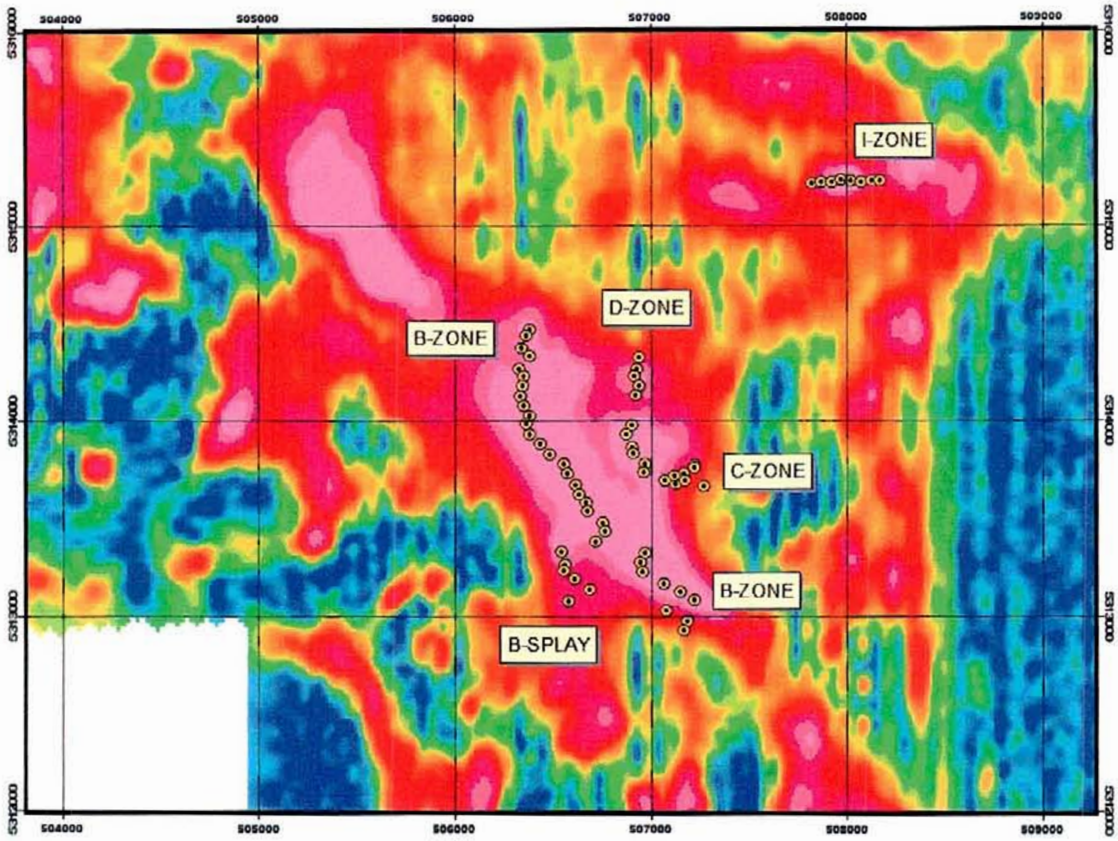


Figure 4. Early off-time EM response for the Bannockburn B-Zone, D-Zone, C-Zone, and B-Zone splay. The B-Zone is defined as a high amplitude, moderate conductance target with a substantial thickness but low conductivity. The thickness of the B-Zone may account for the high apparent conductance as noted in several borehole surveys where modeling is performed using thin plates.

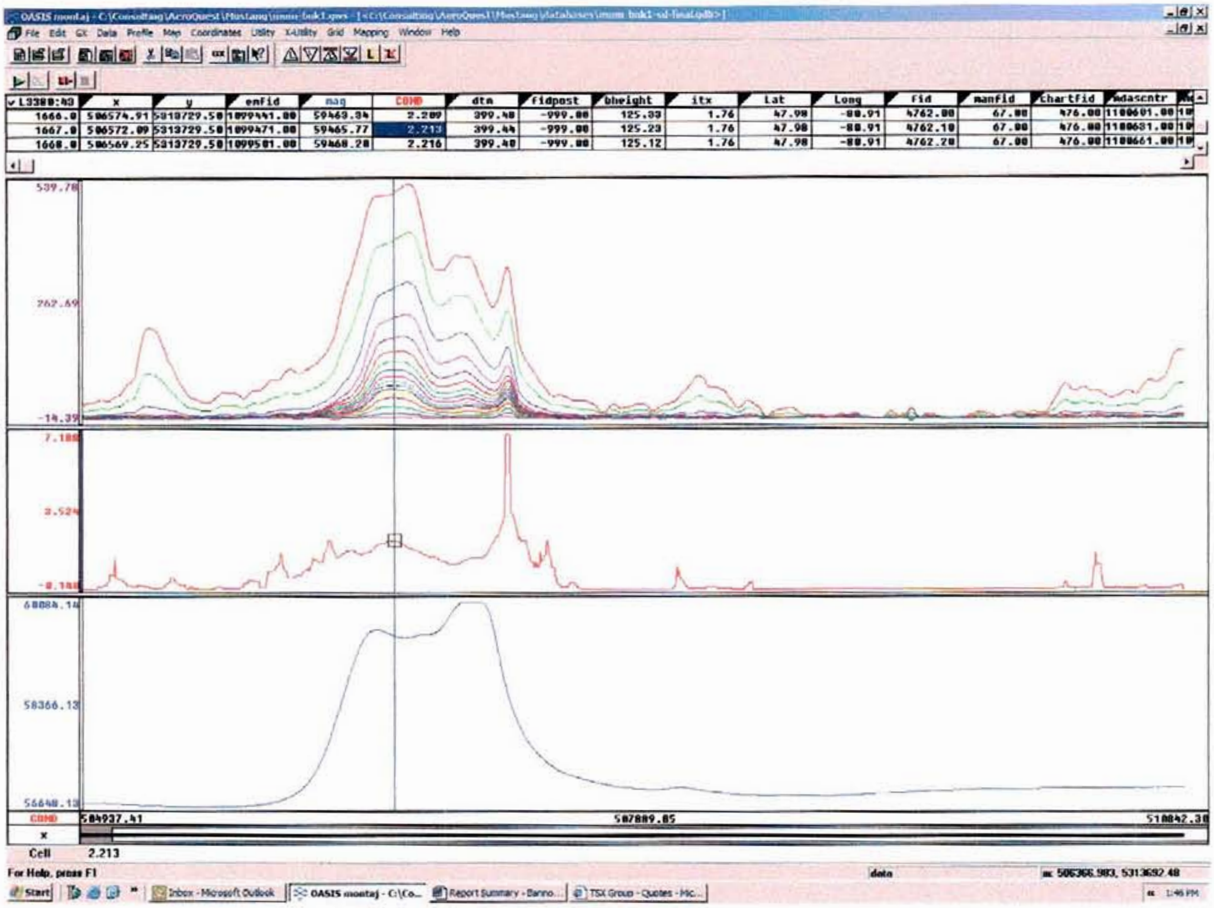

Figure 5. The above AeroTEM Z-axis off-time profiles are typical of the B-Zone. The conductance range is fairly constant from 1-2 S (conductivity range is 0.01-0.05 S/m). The conductor occurs within the ultramafic and there is a close association between higher amplitude magnetic field and conductive response. Note the C-Zone conductor to the east. This target has a higher conductance (7 S) and a much higher conductivity (1-5 S/m). There is no magnetic association with the C-Zone as it occurs outside of the ultramafic.

## APPENDIX 2

Block corner co-ordinates (UTM Zone 17 - NAD27 Canada Mean)

Bannockburn Survey Block Outline (UTM E and N in metres)

| | |
|---|---|
| 504979 5306826 | 504124 5318283 |
| 505036 5313239 | 507829 5318312 |
| 503554 5313210 | 507857 5318654 |
| 503554 5315747 | 510195 5318654 |
| 501644 5315747 | 510195 5318853 |
| 501616 5317286 | 510822 5318882 |
| 500903 5317286 | 511449 5317970 |
| 500875 5318853 | 511449 5317571 |
| 494405 5318853 | 512475 5317599 |
| 494405 5319993 | 512475 5315547 |
| 492638 5320022 | 510622 5315519 |
| 492666 5322559 | 510765 5313153 |
| 497312 5322530 | 511449 5312326 |
| 497312 5322017 | 511506 5309419 |
| 500818 5322017 | 510964 5309305 |
| 500818 5320450 | 510708 5308279 |
| 504095 5320478 | 508484 5308251 |
| | 508456 5306854 |

Claims Listing (The nearby Powell Property, consisting of 4 claims, is described in a separate report)

| Mustang-Outokumpu Option | | | | Mustang Claims 100% | | | |
|---|---|---|---|---|---|---|---|
| Claim | Units | Township | Due Date | Claim | Units | Township | Due Date |
| L1198911 | 8 | BANNOCKBURN | April 11, 2008 | P3009881 | 15 | ZAVITZ | June 25, 2005 |
| L1198912 | 4 | BANNOCKBURN | April 7, 2008 | L3009882 | 14 | HINCKS | June 25, 2005 |
| L1198913 | 1 | BANNOCKBURN | April 7, 2008 | L3016327 | 16 | HINCKS | June 25, 2005 |
| L1198916 | 4 | BANNOCKBURN | April 11, 2008 | L3016328 | 16 | HINCKS | June 25, 2005 |
| L1198917 | 1 | BANNOCKBURN | April 11, 2008 | L3016329 | 16 | HINCKS | June 26, 2005 |
| L1203764 | 1 | BANNOCKBURN | April 11, 2008 | L3016330 | 12 | HINCKS | June 26, 2005 |
| L1206090 | 1 | BANNOCKBURN | April 7, 2008 | L3016331 | 16 | HINCKS | June 26, 2005 |
| L1207453 | 1 | BANNOCKBURN | May 1, 2008 | L3016332 | 8 | HINCKS | June 26, 2005 |
| L1218700 | 2 | BANNOCKBURN | May 15, 2008 | L3016333 | 16 | HINCKS | June 26, 2005 |
| L1218720 | 1 | BANNOCKBURN | March 24, 2008 | L3016334 | 16 | HINCKS | June 26, 2005 |
| L1218721 | 11 | BANNOCKBURN | March 24, 2007 | L3016335 | 16 | HINCKS | June 26, 2005 |
| L1218722 | 6 | BANNOCKBURN | March 24, 2007 | L3012786 | 16 | MONTROSE | June 26, 2005 |
| L1218723 | 1 | BANNOCKBURN | March 24, 2008 | L3000658 | 1 | MONTROSE | June 26, 2005 |
| L1218724 | 1 | BANNOCKBURN | March 24, 2008 | L3012783 | 8 | BANNOCKBURN | June 26, 2005 |
| L1218725 | 7 | BANNOCKBURN | March 24, 2008 | L3012784 | 12 | BANNOCKBURN | June 26, 2005 |
| L1218727 | 7 | BANNOCKBURN | March 24, 2008 | L3012785 | 14 | BANNOCKBURN | June 26, 2005 |
| L1218728 | 1 | BANNOCKBURN | March 24, 2008 | L3005407 | 6 | MONTROSE | June 26, 2005 |
| L1218729 | 2 | BANNOCKBURN | March 24, 2008 | L3005408 | 2 | MONTROSE | June 26, 2005 |
| L1218730 | 1 | BANNOCKBURN | March 24, 2008 | L3012782 | 12 | MONTROSE | June 26, 2005 |
| L1218731 | 1 | BANNOCKBURN | March 24, 2008 | L3005402 | 12 | BANNOCKBURN | June 26, 2005 |
| L1218732 | 11 | BANNOCKBURN | March 24, 2008 | L3005598 | 12 | BANNOCKBURN | June 26, 2005 |
| L1218736 | 1 | BANNOCKBURN | March 24, 2008 | L3005399 | 8 | ARGYLE | June 26, 2005 |
| L1228144 | 8 | BANNOCKBURN | October 15, 2007 | L3005400 | 10 | BANNOCKBURN | June 26, 2005 |
| L1228145 | 16 | BANNOCKBURN | October 15, 2007 | L3005401 | 4 | BANNOCKBURN | June 26, 2005 |
| L1228146 | 16 | BANNOCKBURN | October 15, 2007 | L3011799 | 2 | MONTROSE | Nov. 10, 2005 |
| L1228147 | 8 | BANNOCKBURN | October 15, 2007 | L3011800 | 6 | MONTROSE | Nov. 10, 2005 |
| L1228148 | 6 | BANNOCKBURN | October 15, 2007 | L3011803 | 6 | BANNOCKBURN | Nov. 10, 2005 |
| L1228149 | 6 | BANNOCKBURN | October 15, 2007 | L3011773 | 1 | BANNOCKBURN | Nov. 10, 2005 |
| L1218726 | 1 | MONTROSE | March 24, 2007 | L3011840 | 12 | BANNOCKBURN | Nov. 10, 2005 |
| L1228150 | 8 | MONTROSE | October 15, 2006 | L3011861 | 4 | BANNOCKBURN | Nov. 10, 2005 |
| Total | 143 | | | L3011863 | 12 | BANNOCKBURN | Nov. 10, 2005 |
| | | | | L1167018 | 5 | BANNOCKBURN | Nov 10, 2005 |
| | | | | L1199159 | 12 | BANNOCKBURN | Nov. 10, 2005 |
| | | | | L1199955 | 12 | BANNOCKBURN | Nov. 10, 2005 |
| | | | | L3011885 | 6 | BANNOCKBURN | Nov. 10, 2005 |
| | | | | Total | 356 | | |

Mustang-Phoenix Matachewan Mines Option

| Claim | Township | Due Date |
|---|---|---|
| L1195039 | Argyle | 2004-Oct-31 |
| L1239119 | Argyle | 2005-Apr-30 |
| L1239120 | Argyle | 2005-Apr-30 |
| L1199659 | Bannockburn | 2005-May-31 |
| L1222268 | Bannockburn | 2005-Apr-30 |
| L3002220 | Hincks | 2006-May-17 |
| L3009235 | Hincks | 2005-Jun-25 |
| L3009236 | Hincks | 2005-Jun-25 |
| L1242852 | Montrose | 2004-Oct-31 |
| L3002221 | Montrose | 2006-May-17 |

Patented Claims

| Claim Number | Township |
|---|---|
| MR17999 | Montrose |
| MR18000 | Montrose |
| MR18001 | Montrose |
| L373374 | Montrose |
| L374737 | Montrose |
| L374738 | Montrose |
| L374739 | Montrose |
| L374741 | Montrose |
| L374742 | Montrose |
| L374743 | Montrose |
| L374744 | Montrose |
| L374745 | Montrose |

# APPENDIX 3

Description of Database Fields (Geosoft GDB database)

| Column | Description |
|---|---|
| x | Zone 17 UTM Easting in metres (NAD27-Canada Mean) |
| y | Zone 17 UTM Northing in metres (NAD27-Canada Mean) |
| x83 | Zone 17 UTM Easting in metres (NAD83) |
| y83 | Zone 17 UTM Northing in metres (NAD83) |
| lat | Latitude in decimal degrees (NAD27-Canada Mean) |
| long | Longitude in decimal degrees (NAD27-Canada Mean) |
| lat83 | Latitude in decimal degrees (NAD83) |
| long83 | Longitude in decimal degrees (NAD83) |
| fiducial | Time reference fiducial in seconds |
| manfid | Manual Fiducial |
| chartfid | Chart Recorder Fiducial |
| emfid | Fiducial counter for streaming data synchronisation |
| utctime | UTC Time in seconds of the day |
| rtctime | Local (System) time in HH:MM:SS |
| fltno | Flight number |
| date | Date in YY/MM/DD format |
| galtf | GPS Altitude in metres |
| ralt | Radar Altimeter in metres |
| bheight | Terrain clearance of EM bird in feet |
| dtm | Raw Digital Terrain Model in metres |
| basemag | Base Station magnetic field in nT |
| rawmag | Raw total magnetic intensity in nT |
| mag | Diurnally corrected Total Magnetic Intensity in nT |
| magtie | Final levelled Total Magnetic Intensity in nT |
| x1 | Raw RMS Off-Time EM-X component of channel 1 in ppb |
| z1raw-z6raw | Raw RMS Off-Time EM-Z component of channels 1 to 6 in ppb |
| x1f | Smoothed RMS Off-Time EM-X component of channel 1 in ppb |
| z1f-z6f | Smoothed RMS Off-Time EM-Z component of channels 1 to 6 in ppb |
| ZOn1-ZOn16 | Processed Streaming On-Time Z component Channels 1-16 in nT/sec |
| ZOff0-ZOff16 | Processed Streaming Off-Time Z component Channels 0-16 in nT/sec |
| XOn1-XOn16 | Processed Streaming On-Time X component Channels 1-16 in nT/sec |
| XOff0-XOff16 | Processed Streaming Off-Time X component Channels 0-16 in nT/sec |
| Z1Obr-ZObr16 | Overburden stripped Z component response Channels 1-16 in nT/sec |
| X1Obr-XObr16 | Overburden stripped X component response Channels 1-16 in nT/sec |
| ZOff17-ZOff22 | Special weighted combination channels in nT/sec (see note below) |

| | |
|---|---|
| anum | Index number of conductor pick |
| anomlabel | Letter label of conductor pick |
| nchan | No of off-time (or on-time) channels with response over 2.5nT/sec |
| on_con | On-time conductance in siemens |
| off_con | Off-time conductance in siemens |
| Aclass | Classification from 1-7 based on conductance of pick |
| cond | Interpreted conductance in siemens |

Weighted channels:

ZOff17: 0.25*ch44 + 0.50*ch45 + 0.25*ch46
ZOff18 : (ch46+ch47)/2
ZOff19 : (ch48+ch49+ch50+ch51)/4
ZOff20 : (ch52..ch59)/8
ZOff21 : (ch60..ch75)/16
ZOff22 : (ch76..ch107)/32

In the databases the Survey lines, Tie Lines, and High Altitude/Internal Q coil lines are prefixed with an "L" or "Line", "T" or "Tie", and "S" or "Test", respectively.

**APPENDIX 4** Technical Paper

**Mineral Exploration with the AeroTEM System**
*S.J. Balch, W.P. Boyko, G. Black, and R.N. Pedersen, AeroQuest Limited,* Presented at the SEG Int'l Exposition and 72nd Annual Meeting, Salt Lake City, Utah, October 6-11, 2002

## Mineral Exploration with the AeroTEM System

*S.J. Balch , W.P. Boyko, G. Black, and R.N. Pedersen, AeroQuest Limited.*

#### Summary

AeroTEM is a concentric-loop time-domain EM system designed for mineral exploration and geologic mapping. The high dipole moment of the transmitter in combination with the unique *superimposed dipole* coil geometry allows the system to achieve a depth of exploration similar to fixed-wing systems, but with the resolution and target response symmetry that is typical of conventional helicopter-towed EM systems. AeroTEM has flown over 20,000 line-km since its introduction in 1999. Ground follow-up geophysical surveys and drilling programs have confirmed the depth of exploration to be in excess of 200 m with high spatial resolution of target conductors confirmed. The compact, rigid system geometry should provide for a true on-time measurement of secondary fields from highly conductive sources often associated with Ni-Cu-PGE mineralization, thereby gaining a considerable advantage over all towed-receiver fixed-wing airborne EM systems, which are known to be blind to such targets (Hanneson, 1998).

#### Introduction

Airborne EM systems, as they have evolved since the 1940 s generally fall into one of two categories, namely, (1) the loosely coupled towed-bird systems on fixed-wing aircraft, and (2) the rigid transmitter-receiver configuration towed by helicopters (e.g., Fountain, 1998). The fixed-wing systems operate in the time domain and are characterized by a wideband high-moment transmitter to maximize depth penetration, especially in a resistive environment. The rigid helicopter systems operate in the frequency domain and are characterized by multiple narrow-band low-moment transmitters and closely spaced receivers to maximize spatial resolution and provide moderate depth penetration. Thus one system seeks to maximize signal while the other strives to minimize noise, both attempting to increase the signal-to-noise-ratio...this being the *only* determining factor of an EM system s level of performance.

The AeroTEM system is a wide-band time-domain EM design that draws on the rigid design of the frequency-domain systems and the high-moment transmitter design of the fixed-wing platforms. The system attempts to both maximize signal and minimize noise by incorporating the two major advantages of airborne EM systems transmitter power and rigid coil geometry. As Duckworth (1993) so succinctly states, the optimum coupling to a target by a transmitter-receiver coil pair is achieved by only two possible coil configurations. The first optimum coupling is achieved when the coil separation is 0.6 times the distance to the target the second optimum coupling is achieved when the coils are coincident. Because target depth cannot be known a priori, the coincident coil geometry is obviously preferred.

Figure 1. The AeroTEM airborne electromagnetic system.

#### Method

The system (Figure 1) consists of a 3-axis receiver coil mounted centrally within a large 5-m diameter transmitter loop. The transmitter waveform is a triangular current pulse of 1.15 ms duration at a base frequency of 150 Hz with a peak current of 260 A for a total transmitter moment of 40,000 Am$^2$. The mutually orthogonal receiver coils are mounted with the X-axis along the flight line, transverse, and Z vertical. System waveforms and typical conductor responses are shown in Figure 2.

The system is towed 40 m below the helicopter at a nominal terrain clearance of 30 m. The present transmitter produces a peak primary field of 300 nT vertically below the transmitter at ground level. Because ***bot*** the transmitter and receiver are located close to the ground, AeroTEM produces a stronger target response in the upper 50 m of the earth compared to a fixed-wing aircraft with a peak dipole moment of 500,000 Am$^2$ and a peak primary field of 55 nT at ground surface.

The strength of the primary field from an EM transmitter decreases rapidly with distance from the transmitter location. High moment transmitters on fixed-wing aircraft, such as GEOTEM, tend to have better depth penetration because the strength of the primary field even at 300 m is sufficiently high to energize a conductor and produce a measurable secondary field. Large loop ground EM systems have even greater depth penetration, owing to the lower rate at which the primary field falls off with distance from the transmitter for distances on the order of the loop dimensions. The strength of the primary field from the AeroTEM transmitter is compared with that of some common systems in Figure 3.

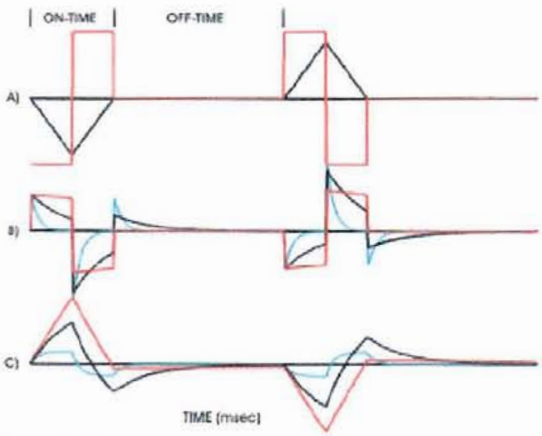


Figure 2. The AeroTEM system is characterized by a) a triangular current pulse at the transmitter and a step response at the receiver. The *dB dt* response in b) and the B-field in c) are shown for conductor time constants of 0.1 ms (blue), 0.5 ms (black) and 5 ms (red).

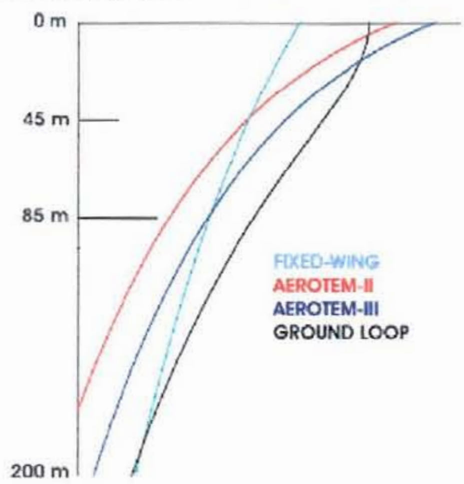


Figure 3: Primary field strength versus depth is compared for fixed-wing ($500{,}000 Am^2$), AeroTEM-II ($40{,}000 Am^2$), AeroTEM-III ($80{,}000\ Am^2$) and ground moving-loop (diameter 100 m, 15 A current, single turn) surface to 200 m.

Although the fixed-wing and ground EM systems gain an advantage in primary field at depth, this energy is diffused over a larger volume, thus reducing their effectiveness in energizing smaller conductors. For large loop ground EM systems, this is especially a problem where large regional conductors can mask the more subtle responses of smaller isolated targets.

**Example One: Spatial Resolution**

The vertical (Z-axis) component produces responses that are independent of the flight line direction. The close proximity of the transmitter and receiver coils produces very sharp anomaly edges. These two factors combine to produce images of the Z component channels that have high spatial resolution.

In the following example, the amplitude of the earliest off-time channel for the Z component receiver coil is shown in Figure 4. The survey was conducted for Nuinsco Resources in the Lac Rocher area of Quebec during an exploration program for Ni-Cu-PGE deposits.

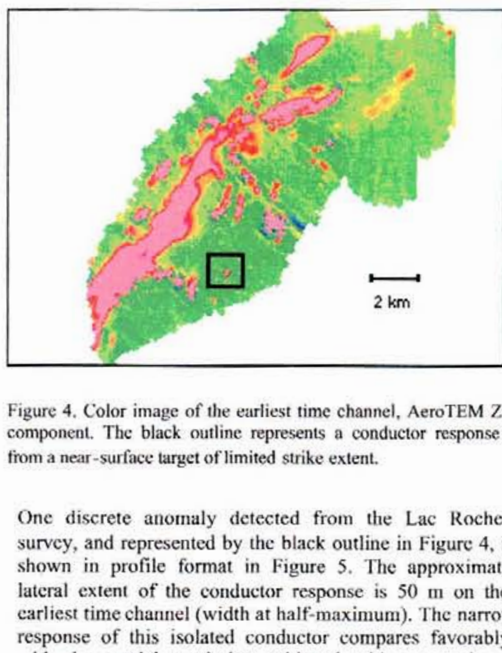


Figure 4. Color image of the earliest time channel, AeroTEM Z component. The black outline represents a conductor response from a near-surface target of limited strike extent.

One discrete anomaly detected from the Lac Rocher survey, and represented by the black outline in Figure 4, is shown in profile format in Figure 5. The approximate lateral extent of the conductor response is 50 m on the earliest time channel (width at half-maximum). The narrow response of this isolated conductor compares favorably with the spatial resolution achieved with conventional HEM systems.

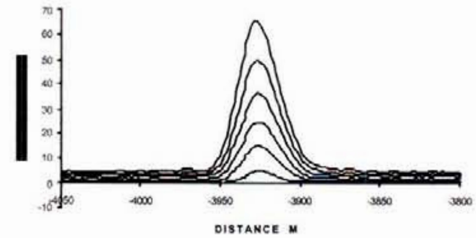


Figure 5: The high spatial resolution of AeroTEM is demonstrated by the EM response of an isolated conductor. The width of the response is less than 50 m on the earliest time channel (peak amplitude at half-maximum).

**Example Two: Air orne - Ground Comparison**

Aurogin Resources, in joint venture with Heron Mines, flew an 800 line-km AeroTEM survey over the Belledune Property in New Brunswick in the search for Cu-Zn-Pb deposits. Several AeroTEM airborne EM conductors were identified from that survey over two separate areas.

A ground follow-up program of Crone Pulse EM was conducted over one selected target in Area Two. The AeroTEM early-time Z component response is shown in Figure 6. The anomaly subjected to the ground follow-up program is outlined in black (Figure 6).

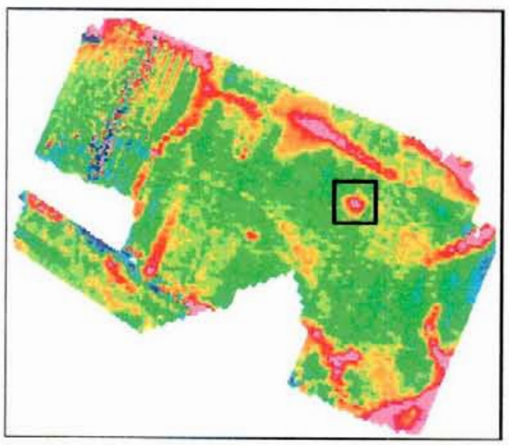

Figure 6: Early-time Z component AeroTEM response over the Belledune Survey Area Two. A detailed ground follow-up survey was centered over the response outlined in black.

An expanded view of the airborne response is shown in Figure 7. The Crone early-time response is shown in Figure 8. The conductor was located within an area of favorable geology. Modeling of the Crone response suggested a sub-horizontal conductor dipping at 25° below the horizontal and located approximately 100 m below surface. The AeroTEM response also suggested a flat-lying conductor because of the symmetric Z component response.

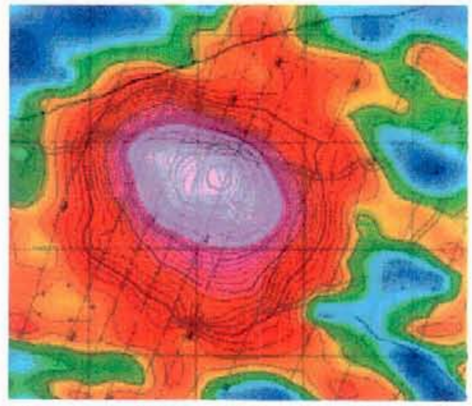

Figure 7: AeroTEM earliest time-channel Z component response, Belledune Property, New Brunswick. The survey was flown with a line spacing of 100 m.

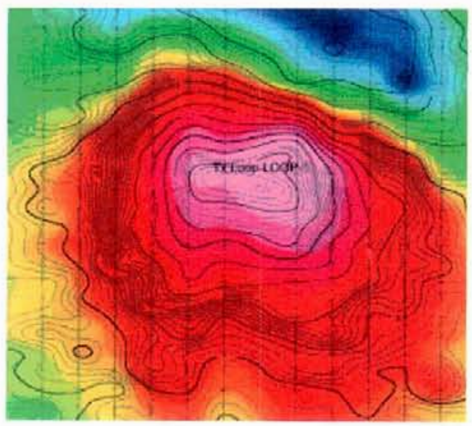

Figure 8: Crone Pulse EM vertical component, ampltide of time channel 10, from the Belledune Property, New Brunswick. The survey was performed in-loop with a 100 m line spacing.

Two boreholes were drilled to then evaluate the EM responses and both intersected up to 15 sulphide containing significant Au-Ag-Cu within a volcanic rhyolite. Downhole Pulse EM surveys confirmed the intersection of a conductor approximately 170 m downhole, coincident with the intersected mineralization, and corresponding to a vertical depth of 145 m. The peak response in the earliest AeroTEM time channel was 90 ppb, or roughly 200 times above the system noise level. The peak response in the Crone survey was 110 nT/s, about 200 times above the system noise level. This is an example of a drilling program that could have proceeded directly from the airborne survey without the added expense of ground geophysics.

**Example Three: Air orne Air orne Comparison**

Nuinsco Resources conducted GEOTEM and AeroTEM surveys over the Lac Rocher property covering both the known mineralized area and a larger area of unexplored claims. In one area of the survey both GEOTEM (Figure 9) and AeroTEM (Figure 10) recorded responses that were coincident with a large magnetic anomaly.

Both systems clearly show a distinct, multi-channel anomaly. Nuinsco drilled the conductor in 1999 and intersected 2.2 m of massive sulphide at a depth of 200 m below surface. The AeroTEM peak response was 3 ppb or 10 times the system noise level, while the GEOTEM peak response was 400 ppm or 40 times system noise level. While noise levels are dependent upon the level of filtering, the higher apparent signal-to-noise-ratio of the GEOTEM response can be attributed to its higher moment transmitter and the depth of the conductor.

**Conclusions**

AeroTEM shows a high spatial resolution, due to its unique coil configuration. The system produces responses that compare well with existing ground and airborne systems. The present depth of exploration is estimated to be up to 250 m with a typical noise level of +/-0.5 ppb.

Improvements to the system will come in the form of larger transmitter moments, decreased noise levels and the development of true on-time measurements through full waveform recording. There are numerous advantages of using helicopter-towed time-domain systems with a depth penetration approaching that of the fixed-wing platforms. The success of these systems will no doubt be dictated by the perceived needs of the mineral exploration industry for such techniques.

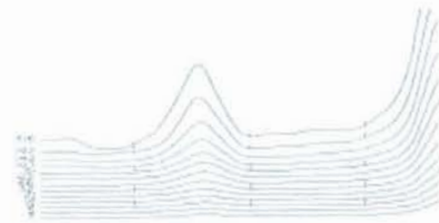

Figure 9: GEOTEM Z component response over a deep conductor at Lac Rocher.

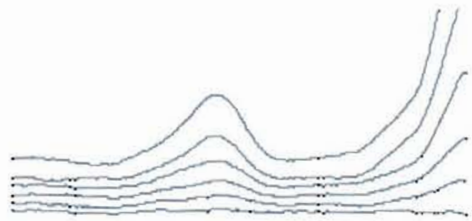

Figure 10: AeroTEM Z component response over a deep conductor at Lac Rocher.

**References**

Boyko, W., Paterson, N.R., and Kwan, K., 2001 AeroTEM characteristics and field results. The Leading Edge, Vol. 20, No 10, pp 1130-1138.

D.K. Fountain, 1998. Airborne electromagnetic systems - 50 years of development. Paper presented at AEM '98 Conference, Sydney, Australia.

K. Duckworth, E.S. Krebes, J. Juigalli, A. Rogozinski, and H.T. Calvert, 1993. A coincident-coil frequency-domain electromagnetic prospecting system. Canadian Journal of Exploration Geophysics, Vol 29. No 2. P 411-418.

J.E. Hanneson, 1998. The effectiveness of airborne EM in Australian mineral exploration a client perspective. Paper presented at AEM '98 Conference, Sydney, Australia.

**Acknowledgments**

AeroQuest wishes to thank Nuinsco Resources and Aurogin Resources for permission to publish the survey data from their respective properties.

**APPENDIX 5** Instrumentation Specification Sheets

**AEROQUEST LIMITED**

**Tel: +1 905 878-5616. Fax: +1 905 876-0193. Email: sales@aeroquestsurveys.com**

# AEROTEM Helicopter Electromagnetic System

### System Characteristics

Transmitter: Triangular Pulse Shape Base Frequency 30 or 150 Hz.
Tx On Time - 5,750 (30Hz) or 1,150 (150Hz) microsec.
Tx Off Time - 10,915 (30Hz) or 2,183 (150Hz) microsec.
Loop Diameter - 5 m.
Peak Current - 250 A.
Peak Moment - 38,800 NIA.
Typical Z Axis Noise at Survey Speed = 8 ppb peak.
Sling Weight: 270 Kg.
Length of Tow Cable: 40 m.
Bird Survey Height: 30 m or less nominal.

### Receiver

Three Axis Receiver Coils (x, y, z) positioned at centre of transmitter loop.
Selectable Time Delay to start of first channel 21.3 , 42.7, or 64.0 msec.

### Analogue Display & Acquisition

Six Channels per Axis.
Analogue (RMS) Channel Widths: 52.9,132.3, 158.7, 158.7, 317.5, 634.9 microsec.
Recording & Display Rate = 10 readings per second.
MDAS Digital recording at 126 sample per decay curve at a maximum of 300 curves per second (26.455 microsec channel width).

### System Considerations

Comparing a fixed wing time domain transmitter with a typical moment of 500,000 NIA flying at an altitude of 120 m with a Helicopter TDEM at 30 m, notwithstanding, the substantial moment loss in the airframe of the fixed wing, the same penetration by the lower flying helicopter system would only require a sixty-fourth of the moment. Clearly the AeroTEM system with nearly 40,000 NIA has more than sufficient moment.

The airframe of the fixed wing presents a response to the towed bird, which must be compensated for dynamically. This problem is non-existent for AeroTEM since transmitter and receiver positions are fixed. The AeroTEM system is completely portable, and can be assembled at the survey site within half a day.

# NEIL FISET
Consulting Geophysicist


## Author's Statement of Qualifications

I, Neil Fiset, of 15 Valley Ridge St., Nepean, Ont., do hereby certify that :

1. I hold a Bachelor of Science degree in Geology(1976) from the University of New Brunswick, Fredericton, New Brunswick.

2. I am a member of the Canadian Exploration Geophysicists Society.

3. Since 1976 I have been an employee of Scintrex Limited, Noranda Exploration Co. Ltd., JVX Ltd. and the United Nations.

5. I have been a self-employed consultant since 1996.

4. I am presently a consulting Geophysicist, practising in Canada and overseas.

5. Permission is granted to Mustang Minerals Corp. to use this report in a prospectus or other financial offering.

6. I have not received, directly or indirectly, nor do I expect to receive any interest, direct or indirect, in the properties of Mustang Minerals Corp. or any affiliate thereof, nor do I beneficially own, directly or indirectly, any securities in Mustang Minerals Corp. or any affiliate thereof

Signed on this 18th day of August, 2004 at Nepean, Ont.

Neil Fiset, BSc.
Consulting Geophysicist


15 Valley Ridge St., Nepean, Ont., CANADA, K2E 7W1
Tel: (613) 228-3214 Fax: (613) 228-9922
email: neifiset@rogers.com